



Super elastic strain limit in metallic glass films

SUBJECT AREAS:

MECHANICAL
PROPERTIES

APPLIED PHYSICS

MATERIALS SCIENCE

PHYSICS

Q. K. Jiang¹, P. Liu^{2*}, Y. Ma¹, Q. P. Cao¹, X. D. Wang¹, D. X. Zhang³, X. D. Han², Z. Zhang^{1,4} & J. Z. Jiang^{1,4}

¹International Center for New-Structured Materials (ICNSM) and Laboratory of New-Structured Materials, Department of Materials Science and Engineering, Zhejiang University, Hangzhou 310027, People's Republic of China, ²Institute of Microstructure and Properties of Advanced Materials, Beijing University of Technology, Beijing 100124, People's Republic of China, ³State Key Laboratory of Modern Optical Instrumentation, Zhejiang University, Hangzhou, 310027, People's Republic of China, ⁴State Key Laboratory of Silicon Materials, Zhejiang University, Hangzhou, 310027, People's Republic of China.

Received
20 July 2012

Accepted
25 September 2012

Published
14 November 2012

Correspondence and requests for materials should be addressed to Q.P.C. (caoqp@zju.edu.cn), X.D.H. (xdhan@bjut.edu.cn) or J.Z.J. (jiangz@zju.edu.cn)

* Contributes equally with the first author.

On monolithic Ni-Nb metallic glass films, we experimentally revealed 6.6% elastic strain limit by in-situ transmission electron microscopy observations. The origin of high elastic strain limit may link with high free volume in the film, causing the rearrangement of loosely bonded atomic clusters (or atoms) upon elastic deformation. This high elastic limit of metallic glass films will shed light on new application fields for metallic glasses, and also trigger more studies for deformation mechanism of amorphous materials in general.

Elastic Strain Limits (ESLs) during tension for most crystalline alloys are less than 1.2%. About 2% ESL were discovered for metallic glasses¹, which are the largest reported value for bulk metallic materials. Hunting new materials with higher ESL are the subject of long-standing interest with potential applications in pressure gauge, spring, sports equipment due to large reversible deformation and mechanical energy storage^{2,3}. Jang and Greer⁴ found the engineering elastic strain of about 3% for the small-sized tensile sample by cut from a Zr-Ti-Co-Be bulk metallic glass. Tian et al.⁵ and Deng et al.⁶ investigated the tensile elastic behavior of small-sized tensile sample fabricated from a Cu₄₉Zr₅₁ glassy ribbon and found engineering elastic strain of about 4.4% for single-bar tensile specimen⁵, and 4.9-5.6% for the framed multiple-bar tensile specimen⁶. Here we report experimental results of 6.6% ESL for monolithic Ni-Nb metallic glass films.

Results

Elastic deformation of Ni-Nb metallic glass film samples were monitored by in-situ TEM images via measuring changes in length and width of samples under tension. Upon gradually heating the copper grid (the bimetallic plates are mounted onto it) in a TEM hot-stage holder with the temperature rise below 100 K, the plates bend, pulling the large frame and the multiple sample bars together (the multiple-bar framed samples are also shown in Fig. S2). To study the elastic strain, the samples were first deformed with only small amount of plasticity but no fracture before unloading. Fig. 1 detailedly depicts the length evolution of four sample bars (labeled as 1-A, 1-B, 1-C, 1-D) during tension. The upper half part of the figure exhibits the length change while the lower half shows the elongation. Upon pulling, all samples extend and exhibit similar behaviors, showing high uniformity for the whole frame-like samples. Hence, representatively, only one series images of sample 1-C were presented in Fig. 2 with gradual length change. The length marked by two vertical red lines tangent to the corner section of the tensile sample are selected to be an apparent gauge length to evaluate the strain. It should be noted that the apparent gauge length defined in such a way leads to a lower bound for the strain measured, since the length change contains the contribution from the regions near the end of the test bar. These regions have slightly larger cross-sectional area and would stretch with a less deformation degree than that in the middle section of the bar. The glassy nature of the tensile samples was confirmed by selected-area electron diffraction (SAED) patterns in the insets of Fig. 2 throughout the tensile tests. The sample has experienced significant elongation (about 14% engineering strain) without shear banding, necking or crystallization (confirmed by SAED in the insets), which reveals the uniform deformation behavior. To distinguish elastic and plastic strains, unloading the sample results in the remarkable elastic shrinkage to only about 4.8% engineering strain accompanied by the increase in width from about 66.2 nm to 70.1 nm. This implies that the sample undergoes 4.8% engineering plastic deformation strain and about 10% engineering elastic strain. Fig. 3 shows the changes in the length and width of tensile sample at different strain stages. The width decreases linearly from about 75.4 nm to 72.3 nm with the elongation of

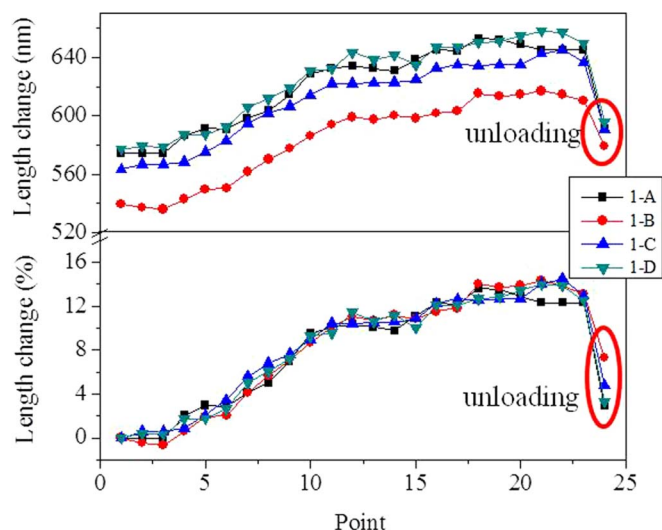


Figure 1 | The length and elongation evolution for four sample bars (labeled as 1-A, 1-B, 1-C, 1-D, respectively) with points where the bright-field TEM images were recorded.

length from about 566.3 nm to 623.4 nm. The ratio of the width change to the length change is estimated to be about 0.37, which is close to the Poisson ratio of Ni-based metallic glass alloys⁷. But it does not mean that the deformation is elastic, since homogeneous plastic deformation can also lead to the similar picture. To confirm the large elastic strain, we further consider the following items:

1. Can the experimental results detected in Fig. 1 be repeated? We repeated the above experiments at least 7 times. Fig. S3 representatively exhibits some analogous results obtained. In all studied Ni-Nb metallic glass films, lengths have experienced significant uniform elongation (about 12~14% engineering strain including both the elastic and plastic strains) without shear banding, necking or crystallization. The loading-unloading data in the Fig. S3 reveal that the samples undergo only 2~4%

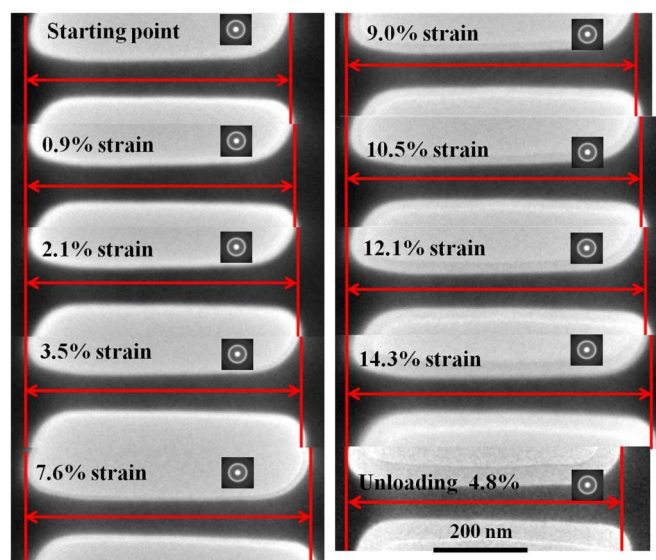


Figure 2 | TEM images of sample 1-C with gradual increasing elongation (the length section with ends marked by two vertical red markers). The corresponding selected-area diffraction patterns of the deformed samples are given in the insets. The shadow on the edges of each image is due to carbon contamination on the sample surface.

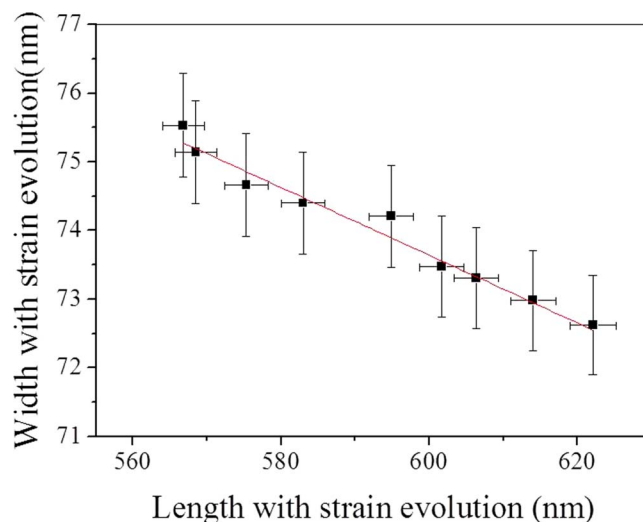


Figure 3 | The average width changes of sample 1-C with length increasing. Along the pulling direction, more than 20 points were count for average.

engineering plastic deformation strain while about 10% engineering elastic strain occurs for monolithic Ni-Nb metallic glass films.

2. Generally, if a material possessing 10% ESL subjected to any tensile strain less than 10%, it would completely recover after unloading. While the tensile strain was above 10%, plastic deformation would occur. Loading-unloading experiments were performed with total engineering strain of 3~5%, 9~11% and 13~15%, respectively. Fig. 4 displays TEM images and length evolutions of sample bars during tension. The samples undergoing 3.7% engineering strain can completely recover and no plastic deformation took place. The sample with 10% engineering tensile strain also suggests the deformation of the sample below 10% may be fully elastic, as unloading leads to the recovery of the sample. When the sample experiences 13.3% engineering tensile strain, remarkable elastic elongation about 9.5% appears accompanied by 3.8% permanent plastic strain. The glassy features of

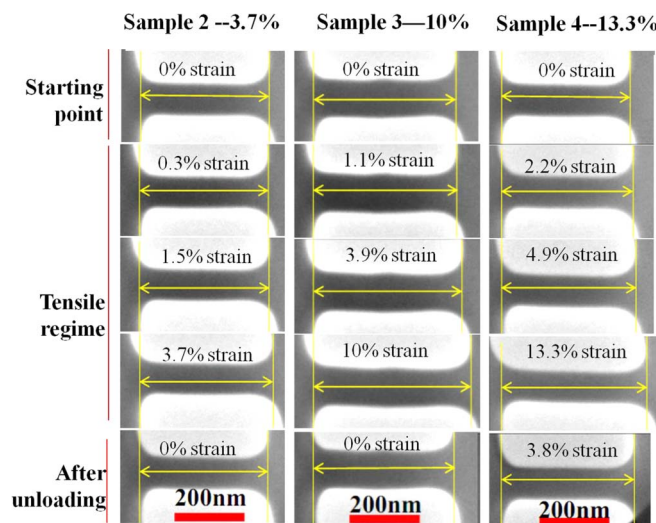


Figure 4 | TEM images for three samples subject to maximum 3.7%, 10.1%, and 13.3% engineering strains, respectively, together with the unloading data.



these tensile samples were confirmed by the zoomed-in bright-field HRTEM images together with SAED patterns. No crystallization was found, as shown in Fig. 5. These results further reveal that monolithic Ni-Nb metallic glass films exhibit excellent elastic deformation ability.

- The sample bars are framed, and the load is transferred to them through the rest of the film which, while of the same thickness, is much larger in other dimensions (Fig. S2). What kind of deformation may occur in the rest of the film as the gauge lengths deform to $\sim 14\%$ engineering strain prior to load release? i.e., does the larger supporting sample affect gauge length measurement upon release? Supposing that no plastic deformation occurs in the larger supporting sample but there is homogeneous plastic elongation in the gauge length. Then, when the load is released, as the surrounding film shrinks back elastically, it would bring the plastically deformed gauge section (and now longer) under near-uniaxial compressive elastic loading. In that case, the measured gauge-length after load release would represent a plastically deformed glass under reverse elastic strain that would mask much of a homogeneous plastic deformation history. However, if the sample confined by frame was stretched to failure, it would become unconfined and no load would be transferred by the frame any more, leading to fully presentation of deformation information. Therefore, tensile deformation up to final fracture allowing clear separation of the elastic and plastic strains should be performed.

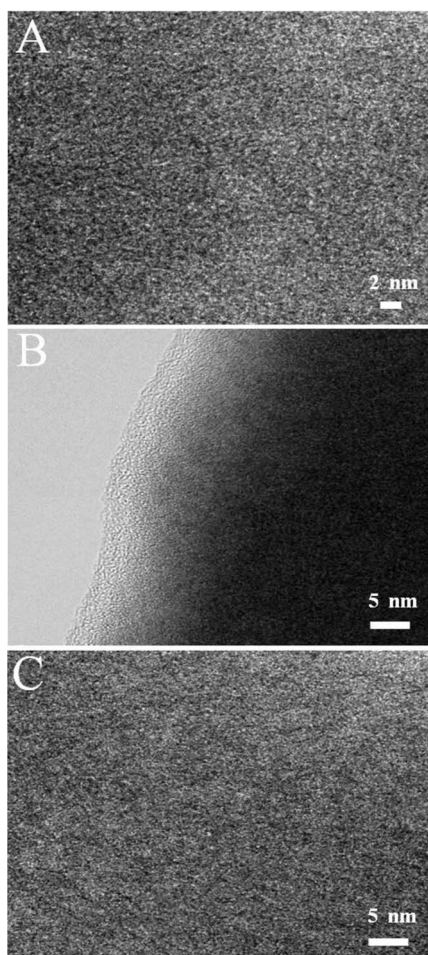


Figure 5 | Zoomed-in bright-field HRTEM images of the tensile sample at different sites.

The evolution of the sample during the tension up to fracture was recorded, as shown in Fig. 6. Contrary to elastic elongation ($\sim 2\%$) followed by catastrophic failure in bulk glassy counterpart, the sample with about 150 nm in width, 50 nm in thickness and 400 nm in length has experienced a large uniform elongation about 59.1% engineering strain before fracture, without shear banding and necking, which makes it relatively easy to evaluate the amounts of the elastic and plastic strains. Fig. S4 exhibits the sample width change versus the length change during deformation, with about 10.4% reduction in the width of the sample over the entire gauge length with 59.1% elongation. Such a linear relation between length elongation and width reduction in the sample further confirms the uniformity of plastic deformation. When the sample was fractured just after 59.1% elongation, it experienced an elastic “shrinkage” of the length and a simultaneous increase of the width from 98.9 nm to 101.2 nm, as can be seen in Fig. 6 and marked in Fig. S4. Putting the two ends of fractured sample together, the plastic deformation experienced by the sample can be estimated to be about 48.9% engineering strain, and the engineering elastic strain about 10.2% is obtained, which was completely recovered after fracture.

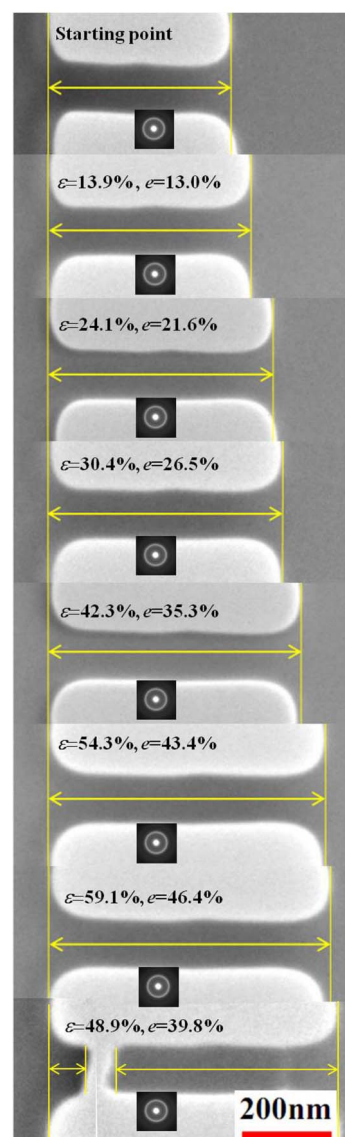


Figure 6 | TEM images of as-sputtered sample extended to fracture. Both of engineering strain (ϵ) and true strain (e) are presented in the figures.



One would notice that the above strain values are “engineering strain ε ”, which is the change in length divided by the original length. However, when the strain is no longer “small” (for example $\varepsilon=10\%$ or more), it is better to use the true strain e , which is the integration of the change in length divided by the instantaneous length from the original length to the instantaneous length, with a relationship between ε and e of $e = \ln(1+\varepsilon)$. Therefore, one can estimate the true elastic strain e of the studied Ni-Nb glassy film based on the engineering strain evaluated from Fig. 6: $e_{\text{elastic}} = e_{\text{totalstrain}} - e_{\text{afterfracture}} = \ln(1+59.1\%) - \ln(1+48.9\%) = 6.6\%$. The 6.6% elastic strain is the highest value ever experimentally reported for a metallic glass.

It should be noted that the engineering elastic strain deduced from loading-unloading of tensile samples without fracture (Fig. 4) is about 10%. If the true strain is adopted, there will be a difference between the engineering and true strains, especially for the larger strain value. For example, one can find that true strain is 9.5% for 10% engineering strain and 12.5% for 13.3% engineering strain, respectively. It indicates that the framed samples probably experienced 2.9% and 5.9% true plastic strain after experiencing 6.6% true elastic strain. After unloading, the sample bars were compressed by frame, according to the experimental results in Fig. 4.

Finally, we estimate the average atomic distance change during tension. It is known that the reverse position for the first maximum diffraction peak in electron or X-ray diffraction patterns correlates with the average atomic distances of metallic glasses with a power law function^{8,9}, and can be conveniently used to roughly estimate the relative change of the average atomic distance of metallic glasses under tension. Here we used the 1/3 power law which is well established for volume estimation of amorphous materials under high temperatures⁹ and pressures^{10–12}. The tension-induced change of the average atomic distance is estimated from the whole diffraction patterns in Fig. S5 to be about 2.0% at the center part of gauge length for the monolithic Ni-Nb metallic glass films under 10% elongation. This means that the strain alone tensile direction should be about $2\% / (1 - 2 \times \text{Poisson ratio}) = 7.7\%$, using the Poisson ratio of 0.37 for the Ni-Nb metallic glass film. This value is consistent with 6.6% ESL (low-bound value) directly deduced from the length change along tensile direction, which confirms that high ESL indeed occurs in the studied Ni-Nb metallic glass film.

Discussion

Elastic behavior is a macroscopic manifestation of atomic bonding, and a result of atomic bond against extension/compression and distortion. Elastic deformations for conventional polycrystalline materials are typically on the order of a few tenths of a percent at most. Only single-crystal whiskers with diameters on the order of micrometers can be deformed in a linear elastic mode up to a strain of about 2% owing to the decrease of structural defects¹³. Further decreasing the sample size, Yue et al.¹⁴ recently revealed large recoverable strain as much as 7.2% in a single-crystal-like Cu nanowire with a diameter of about 5.8 nm by calculating the variation of planar spacing, which was linked with the difficulty to find suitable dislocation sources that can be activated to cause yielding in single-crystal-like Cu nanowire.

Previous works on size effect in metallic glasses at room temperature principally focused on deformation mode, yield/fracture strength and plastic strain achievable^{4,15–18}. It was revealed that the suppression of shear band formation can be obtained by reducing the specimen size^{15–18}. Reducing the diameter of free-standing tensile specimen to nanometer scale, Jang and Greer⁴ found that the Zr-Ti-Co-Be metallic glass deformed homogeneously with the engineering tensile strain of about 6% before necking and fracture, resulting from the suppressed shear banding in small-sized specimen. Under confined testing conditions, tensile ductility can be further enhanced compared with the free-standing uniaxial tension test. For example, Guo et al.¹⁶ found that Zr-Cu-Ni-Al-Ti metallic glass

uniformly elongated up to a engineering tensile strain as high as 15% under confinement, and the total strain reached 45% with obvious necking. This indicates that adding the frame confinement to the loading set-up is also beneficial to the suppression of shear banding and enhancement of plasticity, which is in good agreement with the large plastic strain obtained in Fig. 6. What is the effect of frame confinement on the elastic strain? Recently, Tian et al.⁵ investigated the tensile elastic behavior of Cu-Zr metallic glass using single-bar tensile specimen. They found that the engineering elastic strain is about 4.4%, which is slightly lower than 4.9–5.6% observed by Deng et al.⁶ in the framed multiple-bar tensile specimen with the same composition stretched to fracture. However, after the strain values converted to true strains, one will find the true strains for the Cu₄₉Zr₅₁ glassy ribbons are quite similar ($e=4.3\sim 4.9\%$ for framed multiple-bar sample in Deng et al.⁶ and $e=4.3\%$ for single-bar sample in Tian et al.⁵), not sensitively dependent on the specimen morphology, indicating that the frame confinement on the tensile specimen may not influence the true elastic strain significantly.

For glassy samples, Johnson and Samwer¹ proposed an equation to describe the temperature-dependent shear strain limit, $\gamma_C = \gamma_{C0} - \gamma_{C1} (T/T_g)^{2/3}$, where γ_C is the shear elastic strain limit, γ_{C0} and γ_{C1} are constants. It is clear that if the deformation temperature is fixed at room temperature, the value of γ_C depends only on the glass transition temperature T_g . For Zr-Ti-Co-Be⁴ metallic glass ($T_g=694$ K) and Cu-Zr^{5,6} metallic glass ($T_g=730$ K), the reported engineering elastic strain are about 3 and 4.4%, respectively. The higher T_g the sample has, the larger elastic strain limit can be obtained. Therefore, we selected the Ni-Nb metallic glass as the experimental material due to its higher T_g about 891 K¹⁹ and expect even higher elastic strain limit. This is indeed experimentally observed to be about 6.6% ESL for monolithic Ni-Nb metallic glass film, which far exceeds those observed before in any amorphous metals. What is the origin for such high ESL? We estimate the contribution of linear thermal expansion to elastic strain. Metallic glasses have linear thermal expansion coefficients in the order of $10^{-5}\sim 10^{-6}$ K⁻¹ and the temperature rise during experiments in this work is less than 100 K^{6,20,21}. Thus, linear thermal expansion is only about 0.01%~0.1%²², negligible compared to the 6.6% ESL.

In elastomeric materials like rubbers, the macroscopic reversible extension can be as large as 1000%. Such elastomeric behavior is found in non-crystalline, long-chain polymers, and it requires highly coiled chains which can be stretched straightly under external stress. The ability of chain bending/rotation is crucial to obtain large elasticity of elastomers. Following the idea in non-crystalline polymer, here we propose another factor contributing to the experimentally observed 6.6% ESL of monolithic Ni-Nb metallic glass films. A recent study showed that metallic glasses at room temperature can be perceived as a mixture consisting of atomic clusters and open volume regions²³. The free-volume (or open-volume) model developed by Turnbull et al.²⁴ and applied to the deformation of glass by Spaepen²⁵ is one of the most successful models describing the mechanisms of flow in metallic glasses. When the free-volume content in metallic glass is higher, the atomic jumps are obviously favored since the sites of higher free volume can more readily accommodate local shear, enhancing the ability of deformation. Another viewpoint on the plastic flow in metallic glasses is given by shear transformation zones (STZ) model²⁶. Both models suggest that more fertile sites result in more atomic jump or STZ operation²⁷. It is not unreasonable to consider that Ni-Nb metallic glass films studied in this work contain high degree of flow defects or open volumes due to high cooling rate of the magnetron sputtering fabrication technique. Thus, the fraction of atomic clusters (or atoms) in the vicinity of open volumes is relatively high, which are loosely bonded. Upon elastic deformation, such atomic clusters (or atoms) could be rotated into the tension direction. In other words, the distribution of open volumes in films is rearranged during elastic deformation. Consequently, these

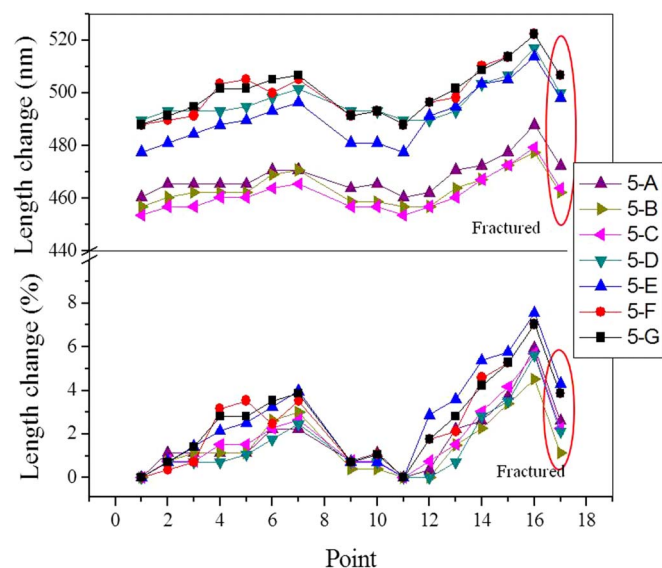


Figure 7 | The length and elongation evolution for several annealed sample bars (labeled as 5-A, 5-B, 5-C, 5-D, 5-E, 5-F, 5-G, respectively).

movements of atomic clusters (or atoms) and open volumes directly result in large macroscopic elongation of the sample. When the tension releases, such atomic clusters (or atoms) and open volumes will be moved back so that the total length of sample can be recoverable.

The most straightforward evidence for high degree of open volume in films comes from the measurements of density change. Therefore, the density of the Ni-Nb metallic glass film prepared by magnetron sputtering was measured, and compared with the density of the Ni-Nb crystalline target for magnetron sputtering. The density of Ni-Nb crystalline material is $8.88 \pm 0.01 \text{ g/cm}^3$ measured according to Archimedes' principle, while the value for the as-sputtered Ni-Nb metallic glass film is $8.50 \pm 0.05 \text{ g/cm}^3$ measured by synchrotron radiation X-ray reflectivity. The density difference between our metallic glass film and the crystalline counterpart is larger than 4%. It is well known that most metallic glasses are slightly less dense than their crystalline counterparts, and the density changes of 0.5–2.0% due to devitrification are typical²⁷. Nagel et al.²⁸ showed that the density of Zr-Ti-Cu-Ni-Be metallic glass increases by $\sim 0.1\%$ upon relaxation, and $\sim 0.8\%$ upon fully crystallization. Density decreases of only $\sim 0.1\text{--}0.2\%$ have been observed upon extensive wire drawing and cold-rolling at room temperature due to the formation of shear bands and excess free volume^{29–31}. Recently, Li et al.³² also revealed that density change upon crystallization in the magnetron-sputtered Cu-Zr metallic glass films were about 3–4%, measured by the cantilever technique. All the experimental results reveal that the open volume content in the magnetron-sputtered Ni-Nb glassy film is high in compared with the metallic glassy ribbon and bulk metallic glass specimen prepared by the conventional melt-spinning and casting techniques, respectively. This experimental result is the evidence to support the model proposed in this work.

To validate the open volume mechanism proposed here, we further experimentally study the ESL of relaxed Ni-Nb glassy sample bars while keeping the sizes and frame confinement unchanged. The relaxed samples were annealed at 523 K for 1 hour in a vacuum below the glass transition temperature of the glass. It is found that the relaxed Ni-Nb glassy sample has a density of $8.64 \pm 0.05 \text{ g/cm}^3$ measured by synchrotron radiation X-ray reflectivity, higher than that for as-sputtered Ni-Nb glassy sample. It is known that annealing treatments at temperatures below the glass transition temperature lead to structural relaxation and the reduction of open volume for metallic glasses^{33, 34}. Fig. 7 depicts the length evolution of the relaxed

samples during in situ tensile test in TEM. After the annealing treatment, the Ni-Nb metallic glass films still remain amorphous state and experienced uniformly elongation (about 5.6–7.0% engineering strain including both the elastic and plastic strains) without any obvious shear banding, necking or crystallization (indicated in Figs. S6–7). The relaxed samples exhibit only 3.1–3.5% engineering elastic strain for monolithic relaxed Ni-Nb films (Here, as the maximal strain value 7.0% is small, the difference between “true strain” and “engineering strain” is negligible). Compared to the as-sputtered samples with 6.6% ESL, these relaxed glassy bars with less content of open volumes exhibit only about 3.1%–3.5% ESL, supporting the open-volume mechanism proposed above.

In summary, about 6.6% elastic strain limit for monolithic Ni-Nb metallic glass films was experimentally revealed by in-situ TEM tension tests. The origin of the high elastic limit is discussed. We propose the rearrangement of loosely bonded atomic clusters (or atoms) upon elastic deformation as a key factor for high ESL. This high elastic strain limit of metallic glass films will shed light on new application fields for metallic glasses, and also trigger more studies for deformation mechanism of amorphous materials in general.

Methods

Ni₆₀Nb₄₀ (at.%) films with thickness of about 50 nm (Fig. S1) were magnetron sputtered on silicon substrate coated with photoresist (etched to be of 2 mm in length and 10 μm in width) by controlling the deposition time of 3 min. The as-sputtered films were transferred by dissolving the photoresist in acetone. Annealing experiments of the as-sputtered Ni-Nb glassy films were performed at 523 K for 1 hour in a vacuum of 2×10^{-3} Pa chamber under purified argon atmosphere. Both of the as-sputtered and as-annealed thin films were adhered to the bimetallic sheets on the 3 mm diameter copper grids and then fabricated to be multi-bar transmission electron microscopy (TEM) samples having widths of about 70–200 nm with window-like frames using focused ion beam machine (FIB). TEM sample preparation is schematically shown in Fig. S2, and experiment details can be found in Refs. 6 and 14 and also in the supplementary section.

- Johnson, W. L. & Samwer, K. A Universal Criterion for Plastic Yielding of Metallic Glasses with a $(T/T_g)^{2/3}$ Temperature Dependence. *Phys. Rev. Lett.* **95**, 195501 (2005).
- Johnson, W. L. Bulk glass-forming metallic alloys: Science and technology. *MRS Bull.* **24**, 42 (1999).
- Inoue, A. Stabilization of metallic supercooled liquid and bulk amorphous alloys. *Acta Mater.* **48**, 279–306 (2000).
- Jang, D. C. & Greer, J. R. Transition from a strong-yet-brittle to a stronger-and-ductile state by size reduction of metallic glasses. *Nature Mater.* **9**, 215–219 (2010).
- Tian, L. et al. Approaching the ideal elastic limit of metallic glasses. *Nature Commun.* **3**, 609 (2012).
- Deng, Q. S. et al. Uniform tensile elongation in framed submicron metallic glass sample in the limit of suppressed shear banding. *Acta Mater.* **59**, 6511–6518 (2011).
- Wang, W. H. Correlations between elastic moduli and properties in bulk metallic glasses. *J. Appl. Phys.* **99**, 093506 (2006).
- Ma, D., Stoica, A. D. & Wang, X. L. Power-law scaling and fractal nature of medium-range order in metallic glasses. *Nature Mater.* **8**, 30–34 (2009).
- Yavari, A. R. et al. Excess free volume in metallic glasses measured by X-ray diffraction. *Acta Mater.* **53**, 1611–1619 (2005).
- Meade, C., Hemley, R. J. & Mao, H. K. High-pressure x-ray diffraction of SiO₂ glass. *Phys. Rev. Lett.* **69**, 1387–1390 (1992).
- Jiang, J. Z., Roseker, W., Sikorski, M., Cao, Q. P. & Xu, F. Pressure effect of glass transition temperature in Zr_{46.8}Ti_{8.2}Cu_{7.5}Ni₁₀Be_{27.5} bulk metallic glass. *Appl. Phys. Lett.* **84**, 1871–1873 (2004).
- Guthrie, M. et al. Formation and Structure of a Dense Octahedral Glass. *Phys. Rev. Lett.* **93**, 115502 (2004).
- Brenner, S. S. Tensile Strength of Whiskers. *J. Appl. Phys.* **27**, 1484 (1956).
- Yue, Y. H., Liu, P., Zhang, Z., Han, X. D. & Ma, E. Approaching the Theoretical Elastic Strain Limit in Copper Nanowires. *Nano Lett.* **11**, 3151–3155 (2011).
- Li, Q. K. & Li, M. Molecular Dynamics Simulation of Intrinsic and Extrinsic Mechanical Properties of Metallic Glasses. *Intermetallics* **14**, 1005–1010 (2006).
- Guo, H. et al. Tensile ductility and necking of metallic glass. *Nature Mater.* **6**(10), 735–739 (2007).
- Volkert, C. A., Donohue, A. & Spaepen, F. Effect of sample size on deformation in amorphous metals. *J. Appl. Phys.* **103**(8), 083539 (2008).
- Kim, J. Y., Jang, D. C. & Greer, J. R. Nanolaminates Utilizing Size-Dependent Homogeneous Plasticity of Metallic Glasses. *Adv. Funct. Mater.* **21**, 4550 (2011).
- Chen, L. Y. et al. Ultrahigh strength binary Ni-Nb bulk glassy alloy composite with good ductility. *J. Alloy & Compd.* **443**, 105–108 (2007).



20. Wang, L. H. *et al.* In Situ Observation of Dislocation Behavior in Nanometer Grains. *Phys. Rev. Lett.* **105**, 135501 (2010).
21. Liu, P., Mao, S. C., Wang, L. H., Han, X. D. & Zhang, Z. Direct dynamic atomic mechanisms of strain-induced grain rotation in nanocrystalline, textured, columnar-structured thin gold films. *Scripta Mater.* **64**, 343–346 (2011).
22. Kato, H., Chen, H. S. & Inoue, A. Relationship between thermal expansion coefficient and glass transition temperature in metallic glasses. *Scr. Mater.* **58**, 1106–1109 (2008).
23. Ye, J. C., Lu, J., Liu, C. T., Wang, Q. & Yang, Y. Atomistic free-volume zones and inelastic deformation of metallic glasses. *Nature Mater.* **9**, 619–623 (2010).
24. Cohen, M. H. & Turnbull, D. Molecular Transport in Liquids and Glasses. *J. Chem. Phys.* **31**, 1164 (1959).
25. Spaepen, F. Microscopic Mechanism for Steady-State Inhomogeneous Flow in Metallic Glasses. *Acta Metall.* **25**, 407–415 (1977).
26. Argon, A. S. Plastic-Deformation in Metallic Glasses. *Acta Metall.* **27**, 47–58 (1979).
27. Schuh, C. A., Hufnagel, T. C. & Ramamurty, U. Overview No.144 - Mechanical behavior of amorphous alloys. *Acta Mater.* **55**, 4067–4109 (2007).
28. Nagel, C. *et al.* Free-volume changes in the bulk metallic glass $Zr_{46.7}Ti_{8.3}Cu_{7.5}Ni_{10}Be_{27.5}$ and the undercooled liquid. *Phys. Rev. B* **57**, 10224–10227 (1998).
29. Deng, D. G. & Lu, B. H. Density change of glassy $Pd_{77}Si_{16.5}Cu_{6.5}$ alloy during cold drawing. *Scripta Metall.* **17**, 515 (1983).
30. Cahn, R. W., Pratten, N. A., Scott, M. G., Sinning, H. R. & Leonardsson, L. Studies of Relaxation of Metallic Glasses by Dilatometry and Density Measurements. *Mater. Res. Soc. Proc.* **28**, 241 (1984).
31. Nasu, T., Nagaoka, K., Itoh, F. & Suzuki, K. Positron Annihilation in Plastically Deformed Ni–P Amorphous Alloy. *J. Phys. Soc. Japan.* **58**, 894 (1989).
32. Li, Y., Guo, Q., Kalb, J. A. & Thompson, C. V. Matching Glass-Forming Ability with the Density of the Amorphous Phase. *Science* **322**, 1819 (2008).
33. Wu, T. & Spaepen F. The relation between embrittlement and structural relaxation of an amorphous metal. *Phil. Mag. B* **61**, 739 (1990).
34. Murali, P. & Ramamurty, U. Embrittlement of a bulk metallic glass due to sub-T_g annealing. *Acta Mater.* **53**, 1467 (2005).

Acknowledgements

The authors would like to thank Shanghai Synchrotron Radiation Source for use of the synchrotron radiation facilities, T.Y. Zhang for discussion of strain estimation from electron diffraction rings, P. Yang and W. Wen for X-ray reflectivity measurements. Financial supports from the National Key Basic Research Program of China (2012CB825700), National Natural Science Foundation of China (Grant No. 10979002, 50920105101, 51071141, 51050110136, 10904127, 11179026, and 11004171), Zhejiang University-Helmholtz cooperation fund, and the Department of Science and Technology of Zhejiang province are gratefully acknowledged.

Author contributions

JZJ designed the whole project. QKJ, PL, YM, QPC, DXZ and XDH carried out the experiments. QKJ, PL, XDW, QPC and ZJJ performed the data analysis, QKJ, QPC, XDW, JZJ, XDH and ZZ discussed the results. QKJ, QPC and JZJ wrote the manuscript.

Additional information

Supplementary information accompanies this paper at <http://www.nature.com/scientificreports>

Competing financial interests: The authors declare no competing financial interests.

License: This work is licensed under a Creative Commons Attribution-NonCommercial-ShareAlike 3.0 Unported License. To view a copy of this license, visit <http://creativecommons.org/licenses/by-nc-sa/3.0/>

How to cite this article: Jiang, Q.K. *et al.* Super elastic strain limit in metallic glass films. *Sci. Rep.* **2**, 852; DOI:10.1038/srep00852 (2012).